(2)

CHEMICAL
RESEARCH,
DEVELOPMENT &
ENGINEERING
CENTER

CRDEC-TR-046

INFRARED SPECTROMETRY OF AEROSOLS

Hugh R. Carlon, U.S. Army Fellow

RESEARCH DIRECTORATE

August 1989

U.S. ARMY
ARMAMENT
MUNITIONS
CHEMICAL COMMAND

Aberdeen Proving Ground, Maryland 21010-5423

Disclaimer

The findings in this report are not to be construed as an official Department of the Army position unless so designated by other authorizing documents.

Distribution Statement

Approved for public release; distribution is unlimited.

UNCLASSIFIED
SECURITY CLASSIFICATION OF THIS PAGE

REPORT DOCUMENTATION PAGE

Form Approved OMB No. 0704-0188

1a. REPORT SECURITY CLASSIFICATION UNCLASSIFIED	1b. RESTRICTIVE MARKINGS
2a. SECURITY CLASSIFICATION AUTHORITY	3. DISTRIBUTION/AVAILABILITY OF REPORT Approved for public release; distribution is unlimited.
2b. DECLASSIFICATION/DOWNGRADING SCHEDULE	
4. PERFORMING ORGANIZATION REPORT NUMBER(S) CRDEC-TR-046	5. MONITORING ORGANIZATION REPORT NUMBER(S)
6a. NAME OF PERFORMING ORGANIZATION CRDEC 6b. OFFICE SYMBOL (If applicable) SMCCR-RSP-P	7a. NAME OF MONITORING ORGANIZATION
6c. ADDRESS (City, State, and ZIP Code) Aberdeen Proving Ground, MD 21010-5423	7b. ADDRESS (City, State, and ZIP Code)
8a. NAME OF FUNDING/SPONSORING ORGANIZATION CRDEC 8b. OFFICE SYMBOL (If applicable) SMCCR-RSP-P	9. PROCUREMENT INSTRUMENT IDENTIFICATION NUMBER
8c. ADDRESS (City, State, and ZIP Code) Aberdeen Proving Ground, MD 21010-5423	10. SOURCE OF FUNDING NUMBERS PROGRAM ELEMENT NO.: PROJECT NO.: 1L161101 TASK NO.: A91A WORK UNIT ACCESSION NO.:

11. TITLE (Include Security Classification)
Infrared Spectrometry of Aerosols

12. PERSONAL AUTHOR(S)
Carlon, Hugh R., U.S. Army Fellow

13a. TYPE OF REPORT	13b. TIME COVERED	14. DATE OF REPORT (Year, Month, Day)	15. PAGE COUNT
Technical	FROM 79 Jan TO 82 Dec	1989 August	39

16. SUPPLEMENTARY NOTATION
Reprinted

17. COSATI CODES		
FIELD	GROUP	SUB-GROUP
17	05	01
20	05, 06	

18. SUBJECT TERMS (Continue on reverse if necessary and identify by block number)
Aerosol spectrometry; Optical scattering; Methodology; SF_6; CCl_2F_2; Water clusters; Spheres; Approximations; Mie Theory

19. ABSTRACT (Continue on reverse if necessary and identify by block number)
Aerosol spectrometry denotes a methodology for describing spectral effects of atmospheric constituents in quantitative, standardized, basic terms. This methodology is based on the premise that most atmospheric constituents can be described (albeit in some cases very unconventionally) as specialized kinds of aerosols, some of which exhibit complex changes in spectral behavior between physical phases. Aerosol spectrometry permits an intuitive understanding of the spectral properties of atmospheric constituents and, very importantly, allows insights not found in traditional or purely mathematical treatments. This report discusses liquid and solid particulate aerosols, special cases including Christiansen effects and isosbestics, and the phase-transitional behavior of liquid droplets in vapor. A study of this behavior led to the finding that anomalous (continuum) infrared absorption in water vapor could be attributed to liquid-like intermolecular hydrogen bonds in molecular complexes (clusters) long before this observation was made using traditional vapor
(continued on reverse)

20. DISTRIBUTION/AVAILABILITY OF ABSTRACT	21. ABSTRACT SECURITY CLASSIFICATION
☒ UNCLASSIFIED/UNLIMITED ☐ SAME AS RPT. ☐ DTIC USERS	UNCLASSIFIED
22a. NAME OF RESPONSIBLE INDIVIDUAL SANDRA J. JOHNSON	22b TELEPHONE (Include Area Code) (301) 671-2914 22c. OFFICE SYMBOL SMCCR-SPS-T

DD Form 1473, JUN 86 Previous editions are obsolete

19. Abstract (continued)

spectrometric techniques. In two appendices, IR spectra are given with absorption coefficients for gases SF_6 and CCl_2F_2, and extinction by nonabsorbing spheres is considered.

PREFACE

The work described in this report was authorized under Project No. 1L161101A91A, Independent Laboratory In-House Research (ILIR) and was performed between January 1979 and December 1982.

The use of trade names or manufacturers' names in this report does not constitute an official endorsement of any commercial products. This report may not be cited for purposes of advertisement.

This document has been approved for release to the public.

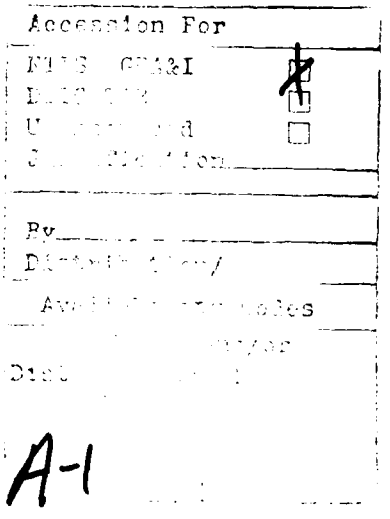

Blank

CONTENTS

LIST OF FIGURES AND TABLES

FIGURES

Table

INFRARED SPECTROMETRY OF AEROSOLS

1. INTRODUCTION

1.1 Background.

Traditionally, infrared (IR) spectrometrists have been concerned with obtaining spectra of homogeneous, single-phase samples. Spectra of gases and liquids are run in gas and liquid cells of known lengths with corrections made for cell window effects, and solids are run, whenever possible, as films or slices of known thickness. Irregular, solid samples are troublesome because they must be immersed in media-like mineral oils (mulls) or compressed salts (pellets), and complex interactions occur between the sample particles and the media, making it very difficult to obtain quantitative spectra. Every effort is made to handle samples in such a way that their absorption spectra are not confused by optical scattering effects and vice versa. It is not surprising, therefore, that the spectrometry of aerosols has always seemed foreboding, that is, something to be avoided. But with the growth in importance of atmospheric optics, especially in the IR, the subject must be addressed. Traditional spectrometrists, on one hand, deal with atmospheric aerosols in conventional terms (e.g., by considering precipitable vapors or droplets in an atmospheric optical path and conceptualizing them as comparable liquid films). On the other hand, applications engineers have developed empirical aerosol models that fit certain situations adequately but are not general and have little or no theoretical basis.

The rapid development and general availability of computers in the past decade have made it possible to use the Mie theory extensively,[1] permitting calculations of aerosol spectral properties that can be verified experimentally. The theory works well for spherical or near-spherical particles, and its use for other particle shapes[2] is being investigated. If traditional spectrometry avoids dealing with aerosols whenever possible, the availability of powerful computer models has exactly the opposite effect. In recent years, a plethora of theoretical papers has appeared, presenting calculations for atmospheric aerosols parametrized in many different ways. Applications engineers are left with three apparent courses of action: (1) to learn and adapt traditional spectrometric techniques; (2) to develop special-case, empirical models because aerosol spectra are easy to obtain but difficult to explain; and (3) to learn the Mie theory and its modeling for many special cases. Understandably, many atmospheric opticists and systems engineers accept the second course of action. This is unfortunate because many classes of aerosol optical behavior are beautifully simple. A methodology is what has been missing between traditional spectrometry and theoretical models that places all aspects of aerosol spectrometry into a meaningful and intuitively satisfying framework. This report presents such a methodology, which has been used successfully at this Center for many years.

As used in this report, aerosol spectrometry denotes a methodology for describing spectral effects of atmospheric constituents in quantitative, standardized, basic terms. An implicit premise in this methodology is that all atmospheric constituents can be described (although it in some cases very unconventionally) as specialized kinds of aerosols, some of which exhibit

complex changes in spectral behavior between physical phases, especially between the vapor and liquid phases. Aerosol spectrometry gives a clear intuitive understanding of the classes of spectra for all kinds of atmospheric constituents and, very importantly, allows insights that would otherwise be impossible by traditional or purely mathematical treatments. Conversely, many classes or cases described for aerosols in this report are immediately recognizable as special ones that can be studied by using existing computational models based on the Mie theory.[3,4]

1.2 Definitions.

Terms used in this report are defined as follows:

α, α_λ = optical extinction coefficient at wavelength λ, m^2/g, or, if subscripted by the scattering component (S) or the absorption component (A) of the extinction coefficient, where $\alpha = \alpha_A + \alpha_S$.

C = mass concentration of particles per unit volume of aerosol, g/m^3.

D_μ = aerosol particle diameter or geometric mean diameter of a distribution, μm.

$f(m_\lambda)$ = correction factor, which depends only on m_λ.

k, k_λ, k_{λ_ν}, k_{λ_L}, k_{λ_s} = imaginary part of the complex index of refraction $(n - ik)_\lambda$, unitless, at wavelength λ if subscripted; also, for the vapor, liquid, or solid phase if subscripted ν, L, or s, respectively; care should be taken not to confuse k_{λ_L} with k_{L_λ}.

k_L, k_{L_λ} = absorption coefficient of material comprising the aerosol particles, μm^{-1}, at wavelength λ if subscripted; care should be taken not to confuse k_{L_λ} with k_{λ_L}.

L = optical path length, m.

λ = wavelength, μm.

M = molecular weight, g/g-mole.

m_λ = complex index of refraction, $(n - ik)_\lambda$, unitless.

$n, n_\lambda, n_{\lambda_v}, n_{\lambda_L}, n_{\lambda_s}$ = real part of the complex index of refraction $(n - ik)_\lambda$, unitless, at wavelength λ if subscripted; also, for the vapor, liquid, or solid phase if subscripted v, L, or s, respectively.

n_θ = mass fraction of water vapor clustered at temperature θ_k.

p = actual vapor pressure, mm Hg.

p_0 = saturation vapor pressure, mm Hg.

$Q, (Q)_\lambda$ = optical cross-section efficiency factor, at wavelength λ if subscripted, unitless.

r_μ = aerosol particle (droplet) radius, μm.

ρ = density of the material comprising the aerosol particles, g/cm^3.

s = saturation ratio or fractional relative humidity, p/p_0, unitless.

t = thickness of an equivalent precipitated film or layer, μm.

T, T_λ = optical transmittance, at wavelength λ if subscripted, unitless.

θ_k = absolute temperature, K.

2. GENERAL THEORY

In the visible region (0.4-0.7 μm), most aerosols extinguish radiation by optical scattering and, except for some carbonaceous or pigmented materials, particle absorption usually is not a significant contributor to the optical extinction coefficient ε. In the submillimeter, millimeter, and centimeter radar regions, atmospheric aerosols extinguish radiation almost entirely by particle absorption. Optical scattering, even by relatively large particles such as water cloud droplets, usually is negligible at these wavelengths. But in the IR and especially in the atmospheric window region at 7-13 μm, optical scattering and particle absorption can both contribute heavily to the overall extinction coefficients observed for common atmospheric aerosols, water fogs, and dusts. At any wavelength λ, the

optical extinction coefficient of an aerosol is the sum of the scattering and absorption components of the aerosol particles:

$$\alpha_\lambda = {}^{\alpha}S_\lambda + {}^{\alpha}A_\lambda \qquad (1)$$

Thus, for most atmospheric aerosols in the visible, ${}^{\alpha}A_\lambda \approx 0$ and $\alpha_\lambda \approx {}^{\alpha}S_\lambda$, whereas in the radar region, ${}^{\alpha}S_\lambda \approx 0$ and $\alpha_\lambda \approx {}^{\alpha}A_\lambda$. But in the IR, ${}^{\alpha}A_\lambda \approx {}^{\alpha}S_\lambda \approx \alpha_\lambda/2$. These conditions correspond, respectively, to those of geometric, Rayleigh-like, and Mie scattering. The classes and conditions are summarized in the Table, where the typical conditions for Mie scattering are greatly simplified for convenience. Actually, as discussed here and in the references, Mie scattering is quite complex.

Table. Classes of Optical Scattering by Aerosols

Class	Popular Name	Typical Conditions	Example
$D_u \ll \lambda$	Rayleigh scattering	${}^{\alpha}S_\lambda \approx 0$ $\alpha_\lambda \approx {}^{\alpha}A_\lambda$	Water cloud in the radar region.
$D_u \approx \lambda$	Mie scattering	${}^{\alpha}S_\lambda \approx {}^{\alpha}A_\lambda$ ${}^{\alpha}A_\lambda \approx {}^{\alpha}S_\lambda \approx \alpha_\lambda/2$	Water fog or dust cloud in the IR.
$D_u \gg \lambda$	Geometric scattering	${}^{\alpha}A_\lambda \approx 0$ $\alpha_\lambda \approx {}^{\alpha}S_\lambda$	Water cloud in the visible.

For aerosol spectrometry, the Beer-Lambert Law is written as

$$\ln (1/T_\lambda) = \alpha_\lambda C L \qquad (2)$$

where the quantitative value of the optical extinction coefficient must be known or determined. Often, atmospheric, aerosol extinction data in literature are reported in units of reciprocal path lengths (km^{-1}, cm^{-1}, dB/km, etc.). This has the effect of combining α_λ and C in equation (2) and severely limits

the value of the data because the kinds, mixing ratios, and size distributions of the aerosol species present when the data were taken must be assumed constant if these data are to be used for subsequent predictive purposes. In aerosol spectrometry, the importance of knowing the optical (mass) extinction coefficients of the aerosol constituents is recognized. These data may be universally applied if airborne mass concentrations and approximate particle size distributions can be determined in any real situation. In this way, the first important characteristic of the methodology is realized: aerosol spectrometry is quantitative.

The second and third characteristics of the aerosol spectrometry methodology are that all atmospheric constituents are described in standardized physical units and that a standard set of terms is used for all constituents, even though, in some cases, these units are highly unconventional. (This is especially true for gases.)

In an earlier paper,[5] the authors show that the equivalent thickness (microns) of a homogeneous precipitated film for a gas or aerosol in an optical path can be expressed as follows:

$$t = (CL)/\rho \qquad (3)$$

where the terms are defined in Section 1.2. For a vapor that behaves like an ideal gas, the mass concentration can be expressed as follows:[6]

$$C = (16\ Mp)/\theta_k \text{ (ideal gas)}. \qquad (4)$$

By combining equations 3 and 4, one can readily see that:

$$t = (16\ MpL)/\rho\theta_k \text{ (ideal gas)}. \qquad (5)$$

For example, for saturated water vapor (M = 18) at 20 °C (p = 17.55), each kilometer (L = 1000) of the optical path contains the equivalent of a layer of precipitable water, t = (16)(18)(17.55)(1000)/(1.0)(293) = 17,251 μm thick, or 1.73 precipitable centimeters of water in the traditional use of the term if water vapor behaves as an ideal gas.

3. PARTICULATE AEROSOLS

In this section, aerosols of liquid and solid particles are considered. While the development is based upon spherical or near-spherical particles, the validity of the Mie theory for particles of other shapes is still being debated.[2] In practice, the techniques presented here work very well for many common atmospheric aerosols.

Many soil-derived dusts[7] and smokes (e.g., sulfuric acid, phosphoric acid, and thermally generated oil smokes)[5] have particle sizes in the atmosphere that are small compared to IR wavelengths (i.e., $D_\mu \ll \lambda$). Most particulate aerosols exhibit this behavior at still longer (radar) wavelengths. These are Rayleigh-like conditions (Table) such that:

$$\alpha_\lambda \approx {}^{\alpha}A_{\lambda}\ (D_\mu \ll \lambda)$$

When optical scattering is negligible, a small particle limit is approached so that:[8]

$$\alpha_\lambda \cdot \rho \approx {}^{\alpha}A_\lambda \cdot \rho \sim {}^{k}L_\lambda \cdot f(m_\lambda) \qquad (D_\mu \ll \lambda) \tag{7}$$

where

$$f(m_\lambda) = \left[\frac{9n}{(n^2 + k^2)^2 + 4(n^2 - k^2) + 4}\right]_\lambda . \tag{8}$$

and it becomes possible to simulate closely (e.g., a liquid droplet cloud by a liquid film). The film can be treated as a sample absorber in an IR spectrometer, and its thickness (micrometer) is given directly by equation 3. For most common aerosol materials, $f(m_\lambda)$ in equation 8 can be taken as 1.0 to a reasonable approximation. For example, for aerosol particulates whose optical constants extend over ranges as broad as $0 \leq k_\lambda \leq 2$ and $0.5 \leq n_\lambda \leq 1.5$, the range of $f(m_\lambda)$ is only $\sim 0.5 \leq f(m_\lambda) \leq 2.0$. Thus, a further approximation is possible for most aerosol materials:

$$\alpha_\lambda \approx {}^{k}L_\lambda / \rho = 4\pi k_\lambda / \lambda \cdot \rho \quad (D_\mu \ll \lambda, \text{ for many common aerosols}) \tag{9}$$

and α_λ may be approximated for equation 2 if only k_λ and ρ are known. Reference 8 gives a detailed discussion of these approximations. Also note that α_λ is a function of $1/\lambda$. Thus, the decrease in α_λ with increasing wavelength for all aerosols is expected and does not necessarily indicate that common aerosols become poorer absorbers at longer wavelengths.

For (spherical) aerosol particles in the Mie or geometric scattering regions (Table), the extinction coefficient is given by:

$$\alpha_\lambda = 3(Q)_\lambda / 2D_\mu \rho \tag{10}$$

where $(Q)_\lambda$ is an optical cross-section efficiency factor or multiplier that typically assumes values of $0 \leq (Q)_\lambda \leq 4$ in the Mie region ($D_\mu \approx \lambda$) and $(Q)_\lambda \approx 2$ in the geometric region ($D_\mu \gg \lambda$).

It is very useful to plot the extinction coefficient of a given aerosol material at a given wavelength as a function of a wide range of particle diameters extending down to the molecular diameters of common substances. Figure 1 shows an example of data measured for a phosphorus smoke aerosol at $\lambda = 10$ μm. Alternatively, the Mie size parameter, D_μ/λ, could be used as the abscissa for similar plots. The dashed curve in Figure 1 extends from the Rayleigh (horizontal section) through the Mie region (small maximum typical of absorbing aerosols) and into the geometric region where it follows the diagonals calculated from equation 10 [specifically the diagonal for $(Q)_{10} = 2.0$]. Thus, Figure 1 shows the behavior of α_{10} at $\lambda = 10$ μm for all possible droplet sizes of this aerosol and includes all three classes of optical scattering summarized in the Table.

The dashed curve in Figure 1 becomes horizontal in the Rayleigh regime ($D\mu \ll \lambda$) at some level given by equations 7 and 8 or approximated by equation 9, where the absorption coefficient and density of the droplets are the primary factors determining α for these nonscattering absorbing droplets.

The interactions between particle absorption and optical scattering are extremely varied for most aerosol materials that are IR absorbers. Superficially, these interactions appear to complicate spectral measurement problems. In reality, the interactions provide kinds of data not attainable by conventional techniques. Many practical applications are discussed in References 5 and 9. Nonabsorbing spherical particles are discussed in Appendix A.

4. VAPORS

In aerosol spectrometry, a vapor is considered a molecular aerosol of the smallest possible particle diameter. This description is highly unconventional but surprisingly useful because it permits, for example, direct comparisons between vapor and aerosol extinctions at a given wavelength. A vapor, observed at any optical wavelength, is the best possible example of a Rayleigh scatterer ($D\mu \ll \lambda$) whose extinction can be assumed due entirely to absorption attributable to modes of interatomic bonds and molecular rotations. The extinction (absorption) coefficients of gases are extremely sensitive to the vapor pressure due to pressure-broadening effects. Therefore, it is always necessary to state the partial pressure for which a given α_λ is reported.[6]* The vapor absorption coefficient increases as partial pressure is reduced, typically reaching some effective maximum < 1 mm Hg.

In IR vapor spectra, the regions of high transparency between absorption bands are often of more interest than the bands. For example, atmospheric gases, including CO_2 and H_2O, define transparent window regions through which most electrooptical systems must operate. These windows vary in transparency in relationship to partial pressures of the gases and to other complex phenomena discussed in Section 6. The band shoulders of atmospheric gases, therefore, are often more important than the absorption peaks.

On a plot for a given wavelength (Figure 1), a pure vapor of a nonpolar liquid could be represented by a single point. This point would be directly above the diameter (molecular) of the vapor molecule on the abscissa and to the right of the vapor absorption coefficient (equations 7 and 8 or approximated from equation 9) on the ordinate calculated for this wavelength. Furthermore, the concept of the vapor-liquid phase transition can be introduced at this point if the vapor is in contact with liquid droplets. (The phase transition will be discussed in detail in Section 6). Thus, the dashed curve would be extended to the right as in Figure 1 to represent the liquid phase (droplets). For example, a liquid aerosol of benzene droplets in air could be

*Freon is a registered trademark of E.I. DuPont de Nemours Company, Wilmington, DE.

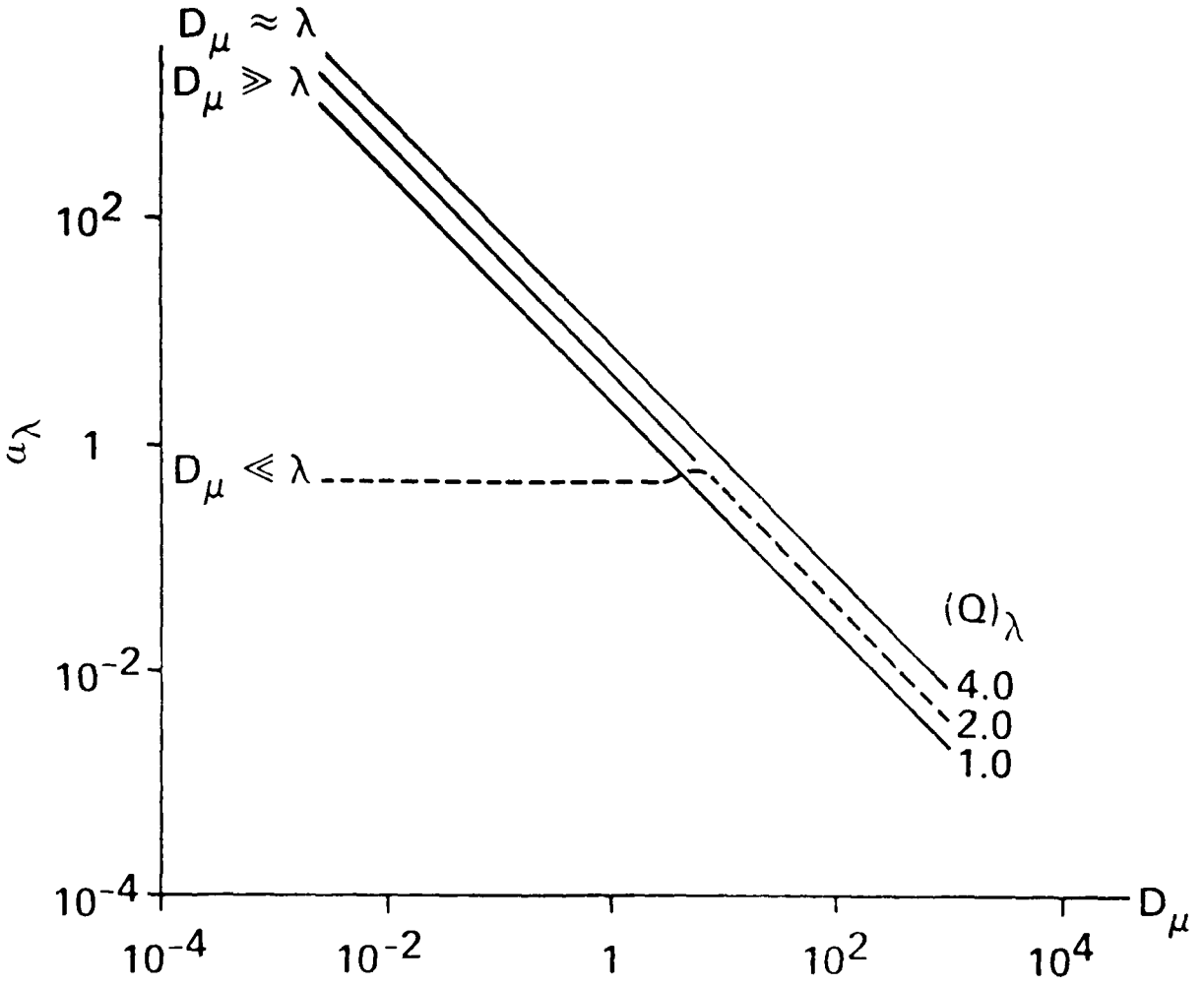

Figure 1. Extinction Coefficient vs. Particle Diameter for Phosphorus Smoke (Dashed Curve) at λ = 10 μm. All three classes of optical scattering from the Table are represented. The solid diagonals are the geometric limits from equation 10.

represented by such a smooth curve, because benzene has the same absorption coefficient in the vapor phase as in the liquid phase at a given wavelength.

Polar substances are not so cooperative as nonpolar ones. For example, liquids and vapors of alcohols have different α_λ.[10] In a plot like Figure 1, the vapor absorption coefficient cannot be shown by a point at the left-hand end (molecular diameter) of the dashed liquid curve because the vapor has a smaller absorption coefficient than the liquid does, and its point lies well below the curve. This behavior invariably indicates intermolecular bonding between molecules in the samples. This circumstance, which will be discussed in detail in Section 6, is very important.

Appendix B gives IR absorption coefficients for the gases SF_6 and CCl_2F_2.

5. SPECIAL-CASE AEROSOLS

5.1 The Christiansen Effect.[11]

The well-known Christiansen effect occurs when a suspension of particles in a transparent medium is observed at a wavelength where the refractive indices of the particles and of the medium are equal, thus producing an optically homogeneous medium with optical bandpass or filter characteristics. Soil-derived, atmospheric dusts and other particulates exhibit the Christiansen effect at IR wavelengths, and their spectra can be simulated by equivalent, precipitated films of the particulates on optical substrates.[11] Useful approximation equations apply at the Christiansen wavelengths that are like those presented in this report for the Rayleigh scattering case. This is because the Rayleigh aerosol particles are too small to scatter appreciably at a given wavelength, whereas the Christiansen aerosol particles at the appropriate wavelengths do not scatter, because their real index matches that of the medium (e.g., air), and all extinction arises from absorption as in the case (approximately) for a Rayleigh aerosol.

Thus, Christiansen aerosols are a special case of a Rayleigh-like class in the Table. The thickness of the precipitated, equivalent film of particulates is given by equation 3, and the approximations of equations 6, 7, 8, and 9 apply. If desired, equation 2 can be written for the Christiansen peak as:

$$\ln (1/T_\lambda) = {}^{k}L_\lambda \cdot t \quad (\text{at } \lambda \text{ Christiansen}) \qquad (11)$$

There are other subclasses of Christiansen behavior in aerosols. For example, some kinds of solid particles in liquid droplets or in other solids can exhibit these effects and might have special applications. Dry, salt particles in air have Christiansen wavelengths and could affect atmospheric transmission spectra.[11] Many kinds of powdered minerals have sharp IR absorption bands and can be used to fabricate optical filters on substrates like polyethylene.[12] Durable and inexpensive Christiansen filters might also be fabricated using such techniques.

5.2 Isosbestics.[13]

Bauman[14] gives an interesting discussion of isosbestics and of "isosbestic points." When only two substances, in equilibrium with each other, are responsible for all absorption in a given wavelength region, at least one point must exist in the spectrum where the absorption coefficient will be independent of the ratio of the concentrations of the two substances. The wavelength at which this occurs is called the isosbestic point or, sometimes, the "isobestic" point. If it can be assumed that the Beer-Lambert Law (equation 2) is applicable, the absence of an isosbestic point is definite proof of the presence of a third constituent.

Isosbestic points (wavelengths) are found in a great many spectra of atmospheric constituents. Hodges[15] shows them near 7.5 and 12.5 μm in spectra of continental and maritime aerosols, and he demonstrates that atmospheric extinction coefficients between these wavelengths are surprisingly independent of the size distributions used for the condensation nuclei. Carlon et al,[5] show that the extinction coefficients of many common smokes and liquid aerosols, including water fogs, are almost independent of droplet size distribution, and that geometric mean diameters may be used in place of diameter distributions with very little effect upon the results obtained. These investigators also show that, at the isosbestic wavelength of 12.5 μm which is found in water and hydrated aerosols like those of Hodges, the aerosol extinc extinction coefficient is completely size-independent from the smallest, possible droplet sizes to droplets as large as about 10 μm, where the geometric limit begins to take effect, and $\alpha_{12.5}$ decreases for larger diameters according to equation 10 where $(Q)_{12.5} = 2.0$. (See Reference 9).

Isosbestics suggest interesting applications that can be studied most conveniently by aerosol spectroscopy. For example, if the complex index of refraction is known for an isosbestic wavelength, it becomes possible to determine remotely the solute concentrations and ratios of chemical equivalents in the droplets, because at this wavelength in equation 2, α_λ is constant and quite independent of droplet-size distribution where the droplet-size distribution is, because of thermodynamic considerations, dependent upon the solute concentration of the droplets! Applications exist where optical extinction at one wavelength could be compared to that at an isosbestic point (wavelength) where the extinction coefficient is a constant. Pure water can be considered the ultimate dilution of solute concentration for hydrated atmospheric aerosols; thus, it is possible to construct a methodology using isosbestic techniques for infinite combinations of solute concentrations and wavelengths.[13]

6. PHASE-TRANSITIONAL AEROSOLS

6.1 Nonpolar Substances.

The concept of the phase transition for the simple evaporation or droplet growth of liquids like benzene was introduced in Section 4. Benzene was used as an example of a substance whose vapor and liquid absorption coefficients are the same at virtually any wavelength and whose behavior could be shown by a plot like Figure 1, where the vapor absorption coefficient could be represented by a point at the left-hand end of the horizontal portion of

the dashed curve (corresponding to the [illegible] diameter). Investigators also noted that polar substances, including alcohols,[10] cannot be plotted like benzene because their points for the vapor absorption coefficients lie below their curves (like the dashed one in Figure 1) for the liquid (droplet) phase.

Only nonpolar substances behave like benzene in this regard. Whenever a vapor point is found (at the molecular diameter as shown in Figure 1) to lie below its liquid curve, this is prima facie evidence that intermolecular bonding exists within the samples and that the intermolecular bonds are active in the absorption at the wavelength of observation.[16] It means that the difference between the vapor and liquid extinction (absorption) coefficients can be attributed to bonds between adjoining molecules that add their absorption to the interatomic modes and rotations of individual molecules in the vapor or liquid. It also indicates that intermolecular bonding, and hence absorption, are functions of the phase density of the sampled material. In nonpolar substances like benzene, intermolecular bonding appears to be negligible regardless of phase density, even for density differences as great as those between vapor and liquid samples.

6.2 Polar Substances.

Probably the most significant insights gained by the aerosol spectroscopy methodology have been those concerning water, especially in the phase transition between the vapor and the liquid. Of all known substances, water exhibits the most pronounced evidence of intermolecular clustering as shown by the ratio of its liquid and vapor absorption coefficients. This ratio can reach 10^3 to 10^4 as shown in Figure 2, where for λ = 10 μm, the liquid absorption coefficient is denoted by $\alpha 10_L$ and the vapor absorption coefficient by $\alpha 10_v$, both for normal ambient temperatures. The error bars on the vapor point show the range of values obtained by many investigators,[17,18] where the value measured is known to vary approximately as the square of water vapor partial pressure or relative humidity.[16]

This simple observation concerning the discrepancy between water's liquid and vapor absorption coefficients, as illustrated in Figure 2, provided evidence that anomalous IR absorption by water vapor could be due to liquid-like, intermolecular (hydrogen) bonding 3 years before similar evidence was found by spectroscopists using conventional vapor techniques.[19,20] In the latter case, this evidence was found in the temperature dependence of the vapor absorption coefficient in steam at wavelengths near the 7-13 μm window region where this anomalous continuum absorption of water vapor is most troublesome. Among vapor spectroscopists, the debate continues to the present as to what molecular-aggregate (cluster) species, if any, could account for the IR continuum absorption of water vapor.[21,22]

Meanwhile, the aerosol methodology has been applied since 1965 to applications and problems associated with atmospheric IR propagation, especially in the 7-13 μm window region, and to the general problem of spectral

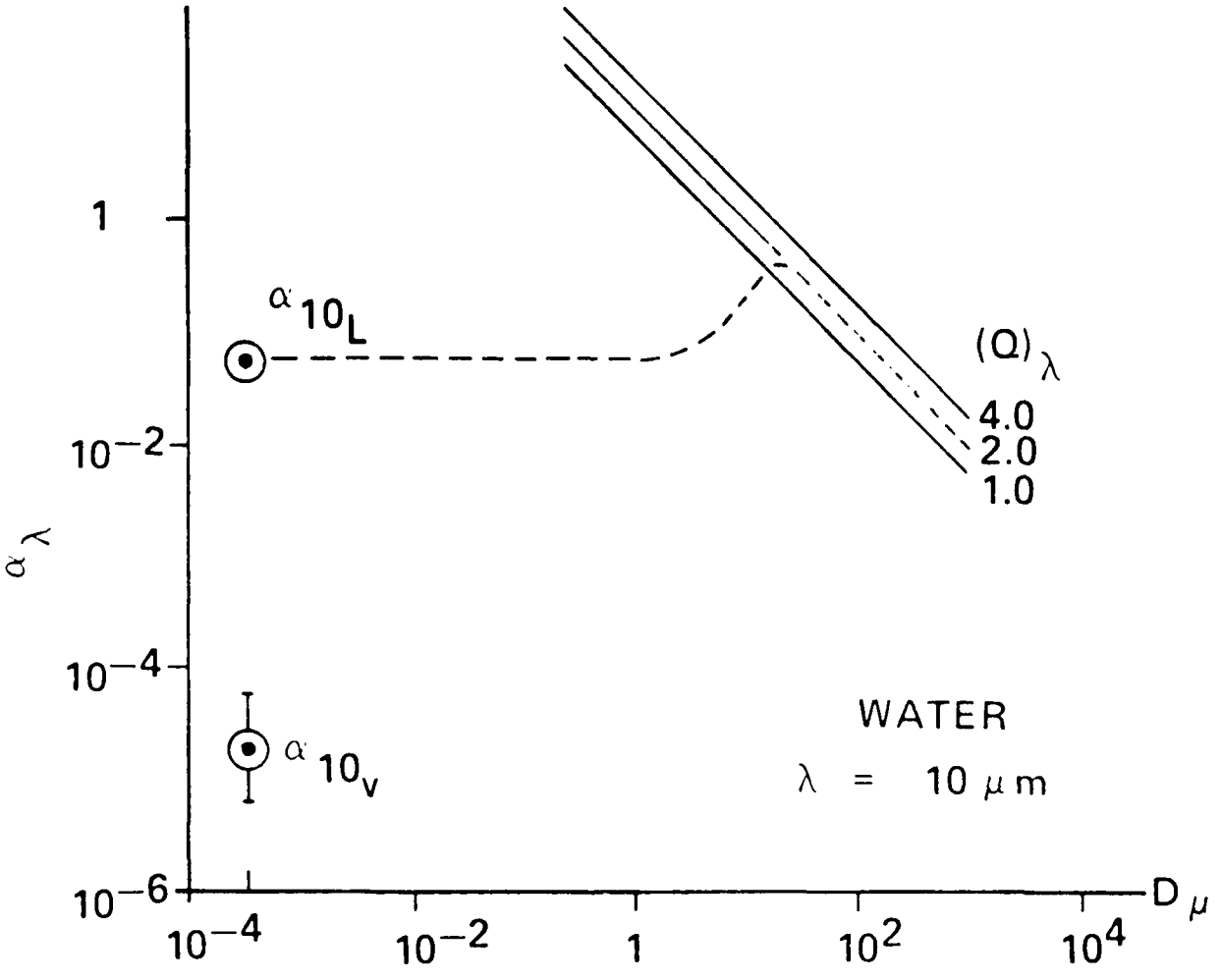

Figure 2. Extinction Coefficient vs. Particle Diameter for Water at λ = 10 μm. Liquid droplets are represented by the dashed curve. At the molecular diameter, the liquid absorption coefficient, α_{10_L}, is 10^3 to 10^4 times larger than the vapor absorption coefficient, α_{10_V}, for normal ambient conditions. This simple observation provides prima facie evidence that intermolecular (hydrogen) bonding occurs in water vapor and liquid and becomes more extensive as the phase density increases through the vapor/liquid-phase transition.

absorption and emission due to clusters of water molecules in the vapor phase that are held together by intermolecular bonds (e.g., hydrogen bonds) or by ionic forces. The earliest applications were concerned with the apparent dependence of terrestrial scintillation (heat wave) intensity upon atmospheric humidity, and the effects of such turbulence upon the operation of IR equipment.[19] This work attributed the modulation to IR absorption by tiny water droplets whose populations were time-varying within the time scale of normal atmospheric turbulence. Because the IR modulation was not accompanied by light scattering in the visible wavelengths, the investigator concluded that these effects were due to water aerosols of submicron radius that are present, or generated, at higher relative humidities (RH). The dependence of the modulation intensity (i.e., "droplet" population) upon the square of the RH also was discussed but, in the absence of knowledge then of what are now called water clusters, this humidity dependency was thought to be due to the growth of the droplets on soluble condensation nuclei. This led to the paradox that if condensation or combustion nuclei were involved, they would be large enough to scatter visible light. But, reduction in visibility did not necessarily accompany intense IR absorption and modulation at higher RH. Thus, existence of a then-unaccounted-for water species in the atmosphere was required to explain all observations. However, this did not deter the application of these findings. Clear-air-turbulence (CAT) detection ahead of aircraft using IR radiometers sensitive to water species was proposed.[23] Recently, success in CAT detection using similar equipment has been reported.[24] An extensive compilation IR atmospheric phenomena that could be attributed to tiny water, aerosol droplets was published,[25] and a model was proposed[26] to explain the IR continuum absorption and other phenomena in terms of fractions of water vapor necessary to be present as liquidlike aerosols to account for the experimental observations. In the retrospect of more recent developments discussed below, the phenomena discussed[19,23,25,26] can now be considered as examples of manifestations of molecular aggregates or water clusters that are always found in the vapor phase.

In a sense, populations of molecular clusters of water monomers individual molecules) in the atmosphere complete the vast family of atmospheric aerosols of all kinds. This concept is illustrated in Figure 3, which is based in part upon work by J. G. Wilson,[27] who summarized the work of C.T.R. Wilson[28,29] and others. The abscissa shows the radius of all species, r_μ in micrometers, while the ordinate shows both the natural logarithm of the ratio of water vapor partial pressure, p, to saturation vapor pressure, p_0, and the saturation ratio or fractional RH (s). The 100% RH or s = 1.0 level is shown as a horizontal line. The growth (with humidity) of all classes of normal atmospheric, condensation nuclei in the Aitken, combustion (continental), and salt (maritime) size ranges is indicated by dashed curves, and this humidity-dependent growth is completely familiar to all atmospheric physicists. At saturation humidity or when slight supersaturation exists, these condensation nuclei grow into haze, fog, or cloud-droplet distributions that have been extensively modeled.[4] These aerosols absorb IR radiation especially at longer wavelength, but they announce their presence by the optical scattering in the visible wavelengths that always accompanies them. Nuclei of this kind were first imagined to be involved in the phenomena reported in reference.[19]

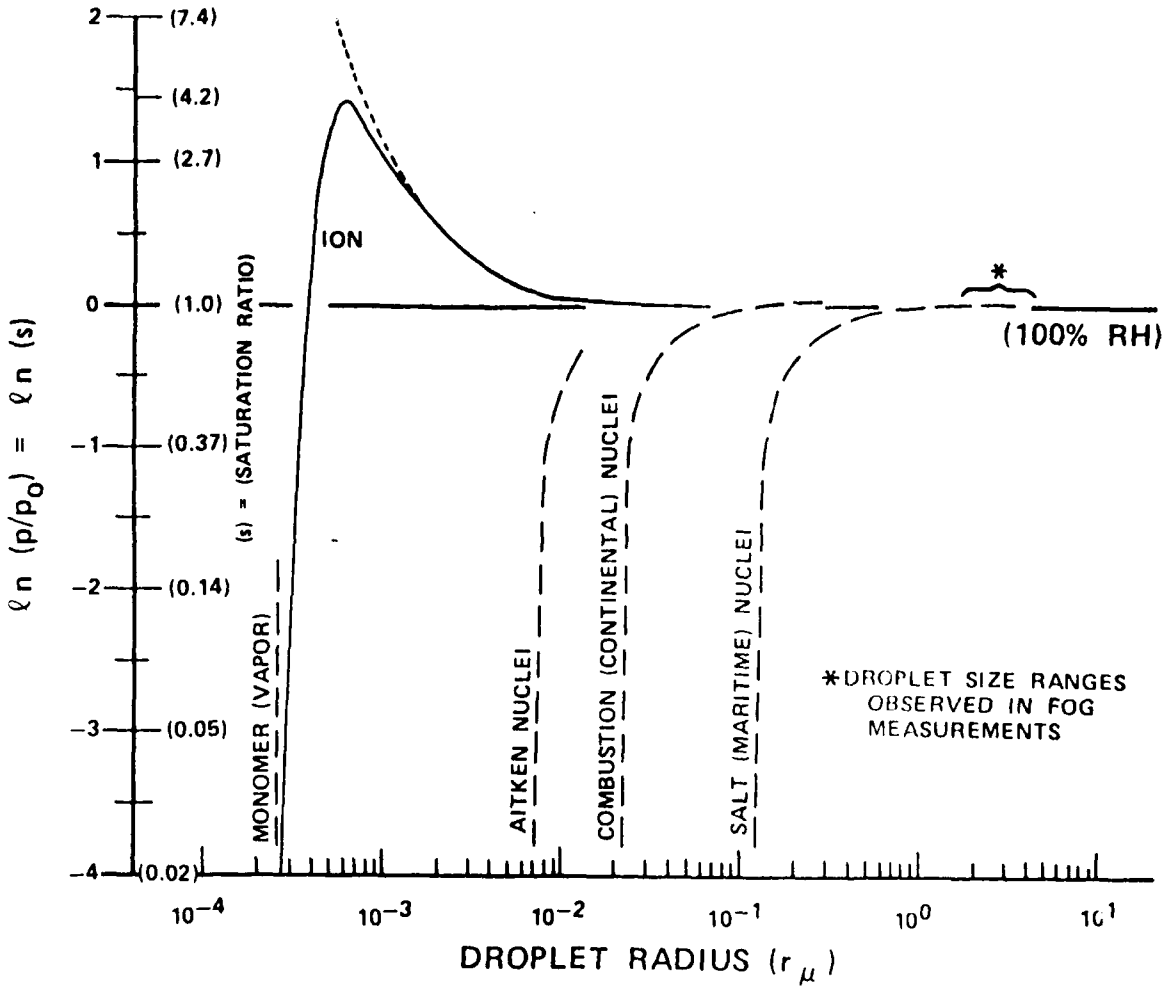

Figure 3. Equilibrium Curves for Atmospheric Aerosols of Many Types at Standard Conditions.[27] The saturation ratio, s, is the fractional RH or ratio of actual-to-saturation vapor pressures, p/p_0. The dashed curves represent classes of nuclei that can grow to visible or near-visible diameters in typical, atmospheric humidity conditions. These condensation nuclei include Aitken, combustion (continental), and salt (maritime) kinds. The peaked, solid curve represents ion hydrates, water ion clusters, or ion-induced neutral water clusters, which are present under normal atmospheric conditions ($s < 1.0$). These clusters cannot grow into droplets large enough to scatter light except when super-saturations of about 4.2 occur. The dotted curve represents homogeneous clusters like the water dimer, which are not expected in real atmospheres because of thermodynamic considerations but for which evidence nevertheless exists.

phase-transitional species between the water monomer (vapor) at its molecular radius and liquid water droplets. This class is shown by the peaked, solid curve labeled ion in Figure 3. These species are ion hydrates or water-ion clusters typically of 10-13 monomers gathered about an ion, and the mean ion cluster size (as can be inferred by the slope of the solid curve in Figure 3) depends directly upon the saturation ratio, s. These ion clusters have modes that correspond to IR wavelengths in the continuum absorption,[16,21] and in moist air, it is possible to measure ion concentrations that have temperature and humidity dependencies similar to those of the IR continuum absorption.[30,31] The ionic charges have very short lifetimes, but water monomers clustered about ions also begin immediately to cross-link with one another by hydrogen bonding. There is a great deal of recent evidence[32,33] that peaked distributions of ion-induced, neutral water clusters are found in water vapor in sufficient numbers to explain the IR continuum absorption. Pronounced evidence is seen in IR emission spectra of steam,[34] under conditions such as those in which vapor spectroscopists first found evidence of intermolecular bonding[20] and, earlier, Elsasser[35] had found an empirical correction to water vapor models to take into account the IR continuum absorption.

In Figure 3, one can see that the peak of the (solid) curve for ion hydrates or ion-induced, neutral water clusters lies near s = 4.2, a supersaturation far larger than that found in normal moist atmospheres. This means that tiny, liquid-like cluster species coexist with larger aerosols in all atmospheres, and that they are able to produce liquid-like IR absorption without growing large enough to scatter visible light - precisely the conditions needed to resolve the paradox discussed earlier. The dotted curve in Figure 3 labeled uncharged represents homogeneous clusters like the water dimer that, because of equilibrium considerations,[27] would be expected to grow immediately into droplets at higher saturation ratios. From the standpoint of aerosol spectrometry, homogeneous species like the dimer are not likely to be able to explain the IR continuum absorption.[21,31,32]

Phase-transitional water (cluster) species of water lend themselves readily to the mass units used in aerosol spectroscopy methodology. Equation 2 is, of course, written for single atmospheric constituents. When more than one constituent is present, equation 2 is written as:

$$\ln (1/T_\lambda) = (\alpha_{1\lambda} C_1 + \alpha_{2\lambda} C_2 + \ldots) (L) \qquad (12)$$

For the case of clusters in water vapor, the monomer concentration from equation 4 can be written $C_1 = (16)(18)(s)(p_0)/\theta_k = 288(s)(p_0)/\theta_k$ if water vapor is taken to be an ideal gas. The mole or mass fraction of water bound in clusters in water vapor, n_θ, is a known function [16] of the saturation ratio such that $n_\theta = K_\theta(s)$. Thus, the cluster concentration in

equation 12 can be written as $C_2 = n_\Theta C_1 = K_\Theta(s)(C_1)$, or equation 12 for water clusters and vapor can be written as:

$$\ln (1/T_\lambda) = 288(s)(p_o)/\Theta_k \cdot \left({}^{\alpha}1_{\lambda} + K_\Theta(s)^{\alpha}2_{\lambda}\right)(L). \qquad (13)$$

That is, the cluster component has an $(s)^2$ dependence like that observed in the IR continuum absorption. A model very similar to the one in equation 13 was given in reference 27, wherein it was shown that in effect, ${}^{\alpha}2_{\lambda}$ could be evaluated directly from the optical constants of bulk liquid water. This is not surprising because water clusters are the phase-transitional species between the vapor and liquid phases. These clusters explain the observations of Figure 2, where ${}^{\alpha}10_{L} = {}^{\alpha}2_{10}$ in equation 13, and ${}^{\alpha}10_{v} = {}^{\alpha}1_{10}$. In other words, the behavior in Figure 2 is due to a mass fraction of $n_\Theta = 10^{-4}$ to 10^{-3} of water clusters floating in the vapor phase.

These observations are intimately associated with investigations of cloud physicists and workers in atmospheric electricity.[30,31,32] Thus, the aerosol spectrometry methodology enables results to be extrapolated to other disciplines where their association might not even be recognized using specialized, traditional, spectroscopic or aerosol modeling techniques. For example, Figure 3 suggests the concept of an IR cloud chamber. Working with visible light, Wilson[28,29] had to obtain critical supersaturation (peak of solid curve labeled ion near s = 4.2 in Figure 3) to grow droplets that he detected by optical scattering. If an IR wavelength or monochromator were used (e.g., near λ = 10 μm, a study of the prenucleation cluster species in real atmospheres should be possible.

7. WORKSHEET

A worksheet for aerosol spectrometry is shown in Figure 4. This worksheet is not intended to include all possible categories of aerosols and possible properties such as birefringence. Rather, the sheet is a starting point for analyzing a given aerosol and its changes with time, temperature, humidity, and other parameters. Changes in k_λ between physical phases have been discussed, especially for the case of the vapor/liquid transition in water (ice and liquid water also show less pronounced but significant phase-transitional differences). The notations in dashed boxes on the worksheet are reminders to investigate this area. One encounters increasing difficulty in applying theory and computational technique as he progresses from the top to the bottom of the worksheet. In most cases, empirical models must be used for nonspherical, solid particulates in the Mie and Rayleigh regions. Additional information is provided in the caption of Figure 4.

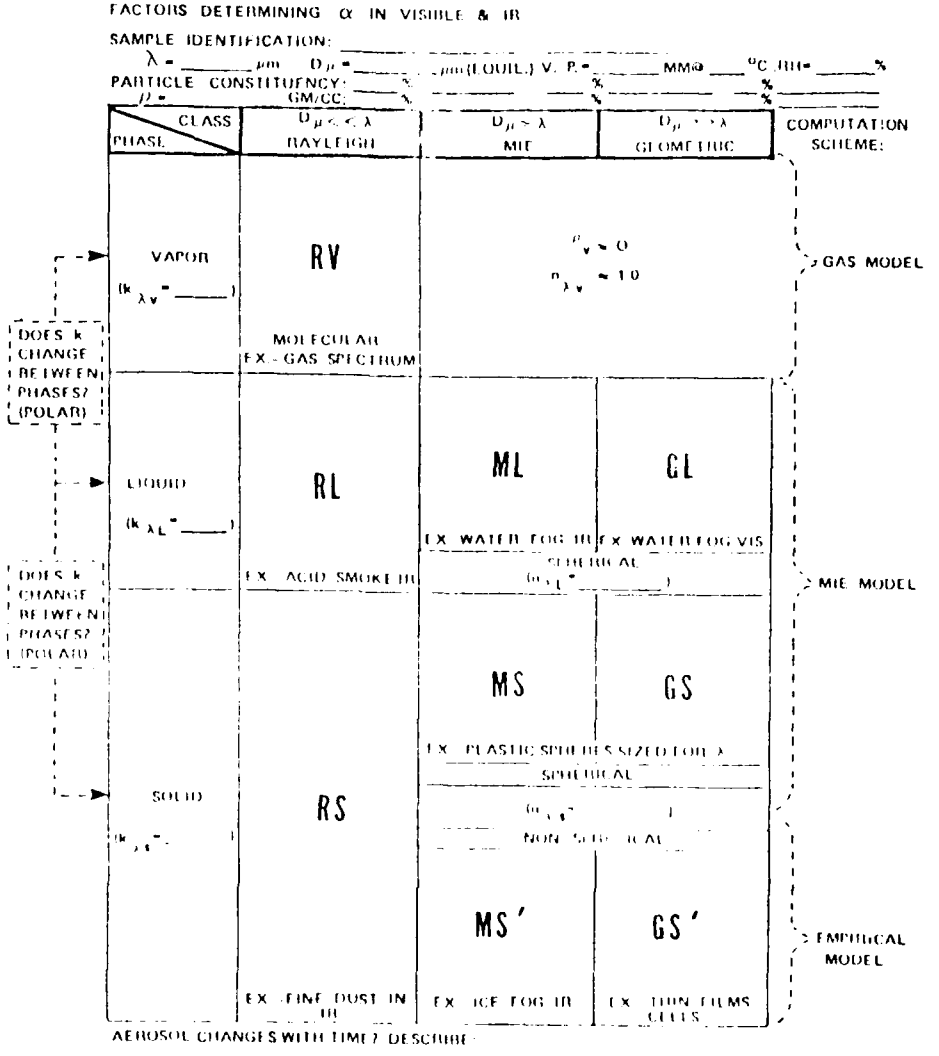

Figure 4. Worksheet for Aerosol Spectrometry. The class/phase designations in bold letters correspond to the optical scattering classes also summarized in the Table: Rayleigh (R), Mie (M), and Geometric (G). The physical phases of the samples are designated in bold letters and in subscripts as vapor (V), liquid (L), and solid (S). The boundary lines between class/phase areas correspond to important changes affecting the extinction coefficient, α, at wavelength, λ. Horizontal boundary lines correspond to phase changes, often with attendant changes in the absorption coefficient or imaginary as well as the real index. Vertical boundary lines correspond to particle growth or size reduction as shown in Figures 1 and 2. For example (from Figure 2), a water fog might begin in class/phase area ML on this worksheet, undergo droplet-size reduction with increased temperature and lowered RH into area RL, and finally evaporate to the gas phase and undergo a major change in the absorption coefficient while entering area RV with an attendant drop in α_{10_V} as shown in Figure 1.

8. CONCLUSIONS

The techniques of aerosol spectrometry are very useful. The purpose of this report has been to set forth the methodology by which these techniques can be applied to the study of many kinds of atmospheric constituents to yield quantitative, standardized descriptions of spectral behavior that are intuitively clear and allow insights that would otherwise be impossible by traditional or purely mathematical treatments. Similar descriptions and units have been used by other authors[36] and are familiar to most atmospheric physicists. A methodology that places all aspects of aerosol spectrometry in an integrated, intuitively satisfying, framework between traditional spectroscopy and theoretical models has been missing. The methodology presented here permits results to be extrapolated to other disciplines such as cloud physics and atmospheric electricity, where the commonality of investigations shared by workers in these fields and atmospheric opticists has been unrecognized or ignored. New results concerned with molecular complexes (clusters) in water vapor show that they are intimately associated with electrical properties of the atmosphere, with atmospheric IR absorption and emission, and with cloud nucleation phenomena. The methodology discussed in this report has been used successfully at this Center for many years and is recommended for consideration and use by applications-oriented systems designers and atmospheric opticists.

LITERATURE CITED

1. G. Mie, Ann. Phys. Vol. 25, p 377 (1908).

2. Acquista, C., "Validity of Modifying Mie Theory to Describe Scattering by Nonspherical Particles," Appl. Opt. Vol. 17, p 3851 (1978).

3. van de Hulst, H.C., Light Scattering by Small Particles, John Wiley, New York, 1957.

4. Deirmendjian, D., Electromagnetic Scattering on Spherical Polydispersions, Elsevier, New York, 1969.

5. Carlon, H.R., Anderson, D.H., Milham, M.E., Tarnove, T.L., Frickel, R.H., and Sindoni, I., "Infrared Extinction Spectra of Some Common Liquid Aerosols," Appl. Opt. Vol. 16, p 1598 (1977).

6. Carlon, H.R., "Infrared Absorption Coefficients (3-15 μm) for Sulfur Hexafluoride (SF_6) and Freon (CCl_2F_2)," Appl. Opt. Vol. 18, p 1474 (1979).

7. Carlon, H.R., "Contributions of Particle Absorption to Mass Extinction Coefficients (0.55-14 μm) of Soil-Derived Atmospheric Dusts," Appl. Opt. Vol. 19, p 1165 (1980).

8. Carlon, H.R., "Practical Upper Limits of the Optical Extinction Coefficients of Aerosols," Appl. Opt. Vol. 18, p 1372 (1979).

9. Carlon, H.R., Milham, M.E., and Frickel, R.H., "Determination of Aerosol Droplet Size and Concentration from Simple Transmittance Measurements," Appl. Opp. Vol. 15, p 2454 (1976).

10. Carlon, H.R., "Quantitative Liquid-Phase Infrared Spectra of Several Simple Organic Compounds," Appl. Opt. Vol. 11, p 549 (1972).

11. Carlon, H.R., "The Christiansen Effect in Infrared Spectra of Soil-Derived Atmospheric Dusts," Appl. Opt. Vol. 18, p 3610 (1979).

12. Carlon, H.R., "Durable Narrow Absorption Band Infrared Filters Utilizing Powdered Mineral Materials on Polyethylene Substrates," Appl. Opt. Vol. 1, p 603 (1962).

13. Carlon, H.R., "Isosbestics in Infrared Aerosol Spectra: Proposed Applications for Remote Sensing," Infrared Physics Vol. 21, p 93 (1981).

14. Bauman, R.P., Absorption Spectroscopy, Vol. 1, pp 419-423, John Wiley, New York, 1962.

15. Hodges, J.A., "Aerosol Extinction Contribution of Atmospheric Attenuation in Infrared Wavelengths," Appl. Opt. Vol. 11, p 2304 (1972).

16. Carlon, H.R., "Phase Transition Changes in the Molecular Absorption Coefficient of Water in the Infrared: Evidence for Clusters," Appl. Opt. Vol. 17, p 3192 (1978).

17. Bignell, K.J., "The Water-Vapour Infra-red Continuum," Quart. J. Roy. Meteorol. Soc. Vol. 96, p 390 (1970).

18. Roberts, R.E., Selby, J.E.A., and Biberman, L.M., "Infrared Continuum Absorption by Atmospheric Water Vapor in the 8-12 μm Window," Appl. Opt. Vol. 15, p 2085 (1976).

19. Carlon, H.R., "The Apparent Dependence of Terrestrial Scintillation Intensity Upon Atmospheric Humidity," Appl. Opt. Vol. 4, p 1089 (1965).

20. Varanasi, P., Chou, S., and Penner, S.S., "Absorption Coefficients for Water Vapor in the 600-1000 cm^{-1} Region," J. Quant. Spectrosc. Radiat. Transfer Vol. 8, p 1537 (1968).

21. Carlon, H.R., "Molecular Interpretation of the IR Water Vapor Continuum: Comments," Appl. Opt. Vol. 17, p 3193 (1978).

22. Watkins, W.R., White, K.O., Bower, L.R., and Sojka, B.Z., "Pressure Dependence of the Water Vapor Continuum Absorption in the 3.5-4.0-μm Region," Appl. Opt. Vol. 18, p 1149 (1979).

23. Carlon, H.R., "Humidity Effects in the 8-13 μm Infrared Window," Appl. Opt. Vol. 5, p 879 (1966).

24. Kuhn, P.M., Nolt, I.G., Radostitz, J.V., and Stearns, L.P., "Infrared Passbands for Clear-Air-Turbulence Detection," Optics Letters Vol. 3, p 130 (1978).

25. Carlon, H.R., "Infrared Emission by Fine Water Aerosols and Fogs," Appl. Opt. Vol. 9, p 2000 (1970).

26. Carlon, H.R., "Model for Infrared Emission of Water Vapor/Aerosol Mixtures," Appl. Opt. Vol. 10, p 2297 (1971).

27. Wilson, J.G., "The Principles of Cloud Chamber Technique," Cambridge Monographs on Physics, University Press, Cambridge, England, 1951.

28. Wilson, C.T.R., "Condensation of Water Vapour in the Presence of Dust-Free Air and Other Gases," Philos. Trans. Vol. 189, p 265 (1897).

29. Wilson, C.T.R., "On the Condensation Nuclei Produced in Gases by the Action of Rontgen Rays, Uranium Rays, Ultra-Violet Light, and Other Agents," Philos. Trans, Vol. 192, p 403 (1899).

30. Carlon, H.R., "Ion Content of Air Humidified by Boiling Water," J. Appl. Phys. Vol. 51, p 71 (1980).

31. Carlon, H.R., "Ion Content and Infrared Absorption of Moist Atmospheres," J. Atmos. Sci. Vol. 36, p 832 (1979).

32. Carlon, H.R., "Do Clusters Contribute to the Infrared Absorption Spectrum of Water Vapor?" Infrared Phys. Vol. 19, p 549 (1979).

33. Carlon, H.R., and Harden, C.S., "Mass Spectrometry of Ion-Induced Water Clusters: An Explanation of the Infrared Continuum Absorption," Appl. Opt. Vol. 19, p 1776 (1980).

34. Carlon, H.R., "Variations in Emission Spectra from Warm Water Fogs: Evidence for Clusters in the Vapor Phase," Infrared Phys. Vol. 19, p 49 (1979).

35. Elsasser, W.M., "Note on Atmospheric Absorption Caused by the Water Rotational Band," Phys. Rev. Vol. 53, p 768 (1938).

36. Jennings, S.G., Pinnick, R.G., and Gillespie, J.B., "Relation Between Absorption Coefficient and Imaginary Index of Atmospheric Aerosol Constituents," Appl. Opt. Vol. 18, pp 1368-1371 (1979).

Blank

APPENDIX A

MASS EXTINCTION COEFFICIENTS ESTIMATED FOR NONABSORBING SPHERICAL AEROSOL PARTICLES IN THE GEOMETRIC SCATTERING REGIME

The Beer-Lambert equation for aerosols can be written as:

$$\ln (1/T_\lambda) = \alpha_\lambda CL \qquad \text{(A-1)}$$

where

T_λ = optical transmittance at wavelength λ (μm)

α_λ = mass extinction coefficient (m^2/g)

C = aerosol mass concentration (g/m^3)

L = optical pathlength (m)

It is straightforward to show[1] that:

$$\alpha_\lambda = 3Q_\lambda / 2D_\mu\rho \qquad \text{(A-2)}$$

where the Mie theory[2] gives the value of Q_λ that depends upon the particle diameter D_μ (μm) compared to the wavelength λ, and ρ is the particle mass density (g/cm^3). In the geometric regime ($D_\mu >> \lambda$), $Q_\lambda \longrightarrow 2.0$ as D_μ increases. Thus:

$$\alpha_\lambda \longrightarrow 3/D_\mu\rho \qquad (D_\mu >> \lambda) \qquad \text{(A-3)}$$

The Figure shows values of α_λ versus D_μ at the He:Ne laser wavelength (λ= 0.63 μm) calculated for spherical droplets of water (dashed curve[3]) and several phthalates (dibutyl-, diethyl-, dimethyl-, and dioctyl- solid curves); the latter are commonly used in aerosol chamber testing.[4] The figure shows that when $D_\mu >>$ 0.63 μm, the Mie-calculated extinction coefficient curves merge into a "tail" whose function is given by equation A-3 and whose thickness depends mainly upon the differences in mass densities (ρ) of the liquids that are represented. The density differences are not obvious because of the logarithmic scale used for the ordinate of the Figure. A great many liquid and solid substances exist for which, when they are dispersed as spherical particles at wavelengths where their absorption is negligible, remarkably good first approximations of α_λ can be made using equation A-3. Hence, equation A-3 is a useful one for first calculations involving such

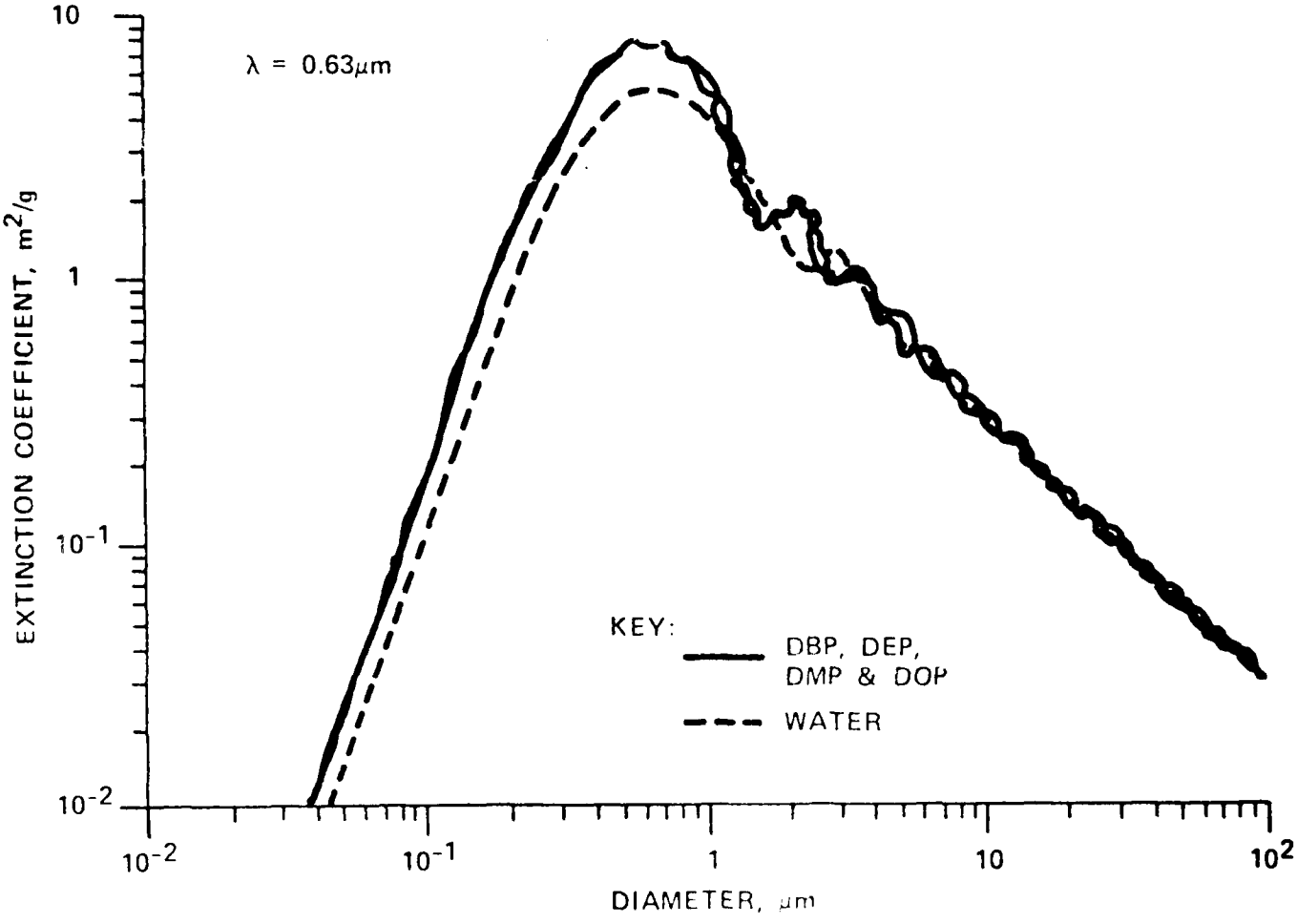

Figure. Mie-Calculated Extinction Coefficient vs. Spherical Droplet Diameter for the He:Ne Laser Wavelength (λ = 0.63 μm). The dashed curve is for water droplets, whereas the solid curves are for droplets of several kinds of phthalates (dibutyl, diethyl, dimethyl, and dioctyl).

aerosols when their optical properties are not known at some wavelength λ, but $D_\mu >> \lambda$. A common example is that of water-fog droplets in the visible wavelengths. Often, visible-wavelength observations can be combined with infrared (IR) measurements to yield additional information about an aerosol (e.g., mean particle diameter).[5] Combining equations A-1 and A-3 gives:

$$\ln (1/T_\lambda) = 3/D_\mu \cdot \rho \quad CL \qquad (D_\mu >> \lambda) \qquad (A\text{-}4)$$

and it is straightforward to show that:

$$\ln (1/T_\lambda) = \pi/2 \quad D_\mu^2 \cdot N \cdot L \cdot 10^{-6} \qquad (D\mu >> \lambda) \qquad (A\text{-}5)$$

where N is the number of spherical particles per cubic centimeter. Equation A-5 can be extended to some rather practical applications. For example, Middleton[6] estimates meteorological range as that for which a high-contrast target is seen with 2% transmittance, that is, $T_\lambda = 0.02$ and $\ln (1/T_\lambda) = 3.912$ so that equation A-5 can be written as:

$$N = 2.49 \cdot 10^6/D_\mu^2 \cdot L \qquad (D_\mu >> \lambda) \qquad (A\text{-}6)$$

As an example, a typical, developing water fog is comprised of droplets having mean diameters in the 3-5 μm range. If an observer could barely see a high-contrast target at L = 200 m under such conditions, from equation 6, the fog should contain approximately 500-1400 droplets per cubic centimeter. Perhaps a more useful application would be to calculate mean values of D_μ from equation 6 using observed ranges (L) and droplet populations (N) measured by independent means as a water fog aged and dissipated.

LITERATURE CITED

1. Carlon, H.R., "Practical Upper Limits of the Optical Extinction Coefficients of Aerosols," Appl. Opt. Vol. 18, p 1372 (1979).

2. G. Mie, Ann. Phys. Vol. 25, p 377 (1908).

3. Carlon, H.R., Anderson, D.H., Milham, M.E., Tarnove, T.L., Frickel, R.H., and Sindoni, I., "Infrared Extinction Spectra of Some Common Liquid Aerosols," Appl. Opt. Vol. 16, p 1598 (1977).

4. Carlon, H.R., Kimball, D.V., and Wright, R.J., "Laser Monitoring of Mass Concentrations of Monodisperse Test Aerosols," Appl. Opt. Vol. 19, p 2366 (1980).

5. Carlon, H.R., Milham, M.E., and Frickel, R.H., "Determination of Aerosol Droplet Size and Concentration from Simple Transmittance Measurements," Appl. Opt. Vol. 15, p 2452 (1976).

6. Middleton, W.E.K., Vision Through the Atmosphere, p 105, University of Toronto Press, Canada, 1952.

APPENDIX B

INFRARED ABSORPTION COEFFICIENTS (3-15 μm) FOR SULFUR HEXAFLUORIDE (SF_6) AND FREON* (CCl_2F_2)

B-1. INTRODUCTION

It is well known that Freon™* (CCl_2F_2) and sulfur hexafluoride (SF_6) are gases with strong absorption in the infrared (IR). For example, they can be used for wavelength calibration of spectrometers or scanning radiometers or in atmospheric tracer studies. Many workers are also aware that SF_6 has a very strong absorption peak that overlaps the CO_2 laser lines near 10.6 μm. The extinction (absorption) of these gases is seldom discussed in literature of IR applications. Yet, these data are of potential importance to workers, for example, in the fields of atmospheric or aerosol spectroscopy. The purpose of this report is to present absorption data for these gases in mass absorption coefficients that can be, for example, compared directly to aerosol extinction coefficients and to suggest practical applications of these data.

The general expression for the mass concentration $C(g/m^3)$ of an ideal gas at pressure p(mm Hg) is:

$$C = 16Mp/\theta_k \qquad \text{(B-1)}$$

where the new, and all subsequent, terms are defined in the glossary of this appendix. To facilitate direct comparison of the absorption coefficients of gases to the extinction coefficients of aerosols, they can both be expressed in mass units at a given wavelength, λ, in Beer-Lambert law:

$$\ln (1/T_\lambda) = \alpha_\lambda C L_m \qquad \text{(B-2)}$$

For aerosols, α_λ is usually considered to be a constant at some wavelength. But in reality, α_λ is a function of other parameters that must also be specified. For example, the scattering component of α_λ is affected by particle shape, size distribution, and bulk density. For liquid droplets, α_λ is affected by a solute concentration that, for water-based droplets, is dependent upon humidity.[1] For gases, α_λ is a strong function of sample pressure, p, (or of partial pressure, as for gases mixed with atmospheric air). Vapor pressure has no direct counterpart in the condensed aerosol phases. Pressure-broadening of gas absorption bands is well known and widely studied. If desired, investigators can apply corrections for pressure (or temperature) to spectra presented in this report.

*Registered Trade Mark of E.I. Du Pont de Nemours & Company, Incorporated, Wilmington, DE.

B-2. EXPERIMENTAL PROCEDURE

Sulfur hexafluoride spectra were taken at 25 °C by Lagemann and Jones.[2] Sample purity was greater than 98%. Possible contaminants were F_2, HF, H_2O, and sulfur fluorides, but only traces of SF_4 were found. Spectra were run using a Perkin-Elmer Model 21 spectrometer. A 10-cm long sample cell with KBr windows was used for the measurements reported here. Spectra were recorded at SF_6 pressures of 762, 25.4, and 1.6 mm Hg. The cell was sealed to exclude atmospheric air.

Freon spectra were taken by the author[3] at 25 °C in a 10-cm cell with NaCl windows. The partial pressure, p, was 4.2 mm Hg in air at 1 atm total pressure. The sample was aerosol-can propellant identified on its label as dichlorodifluoromethane (CCl_2F_2) and used as a freezing spray without added solutes for electronic applications.

Because the value of α_λ is highly dependent upon the pressure of a gas sample due to pressure-broadening, the values of SF_6 herein reported are for three pressures, including the lowest one given in reference 2 (1.6 mm Hg), which yields the maximum values of α_λ for these data. For Freon™, only one partial pressure taken in air at 1 atm total pressure was available, and comparative extinction coefficients at different pressures could not be calculated. However, the sample pressure (4.2 mm Hg) was comparable to the lowest SF_6 partial pressure used (1.6 mm Hg).

B-3. RESULTS AND DISCUSSION

Figure B-1 summarizes α_λ for gas pressures of 762, 25.4, and 1.6 mm Hg of SF_6. Figure B-2 shows α_λ for CCl_2F_2 at a partial pressure of p = 4.2 mm Hg. The peak values are 2.4 m^2/g at λ = 10.64 μm for pure SF_6 at 1.6 mm Hg, and 1.2 m^2/g at λ = 11.8 μm for CCl_2F_2 at 4.2 mm Hg in atmospheric air.

Taken together, these two gases used in conjunction with an isotopic CO_2 laser near 10.6 μm would produce intense absorption by SF_6 on the one hand (α_λ = 1 - 2 m^2/g at 1.6 mm Hg) and relatively high transparency for Freon™ on the other (α_λ ≈ .03 m^2/g).

The peak absorption coefficients reported here for Freon™ and SF_6 are substantially larger than coefficients of acid smokes in this wavelength region. For example, phosphorus smoke gives a value of α_λ = 0.4 m^2/g at λ = 8.0 μm and 9.8 μm, whereas H_2SO_4 mists or smokes give α_λ = 0.5 m^2/g at λ = 8.4 μm. The value of α_λ for typical liquid, water fogs rises from about 0.05 m^2/g to about 0.34 m^2/g over the wavelength interval from 7 to 15 μm.[1,3]

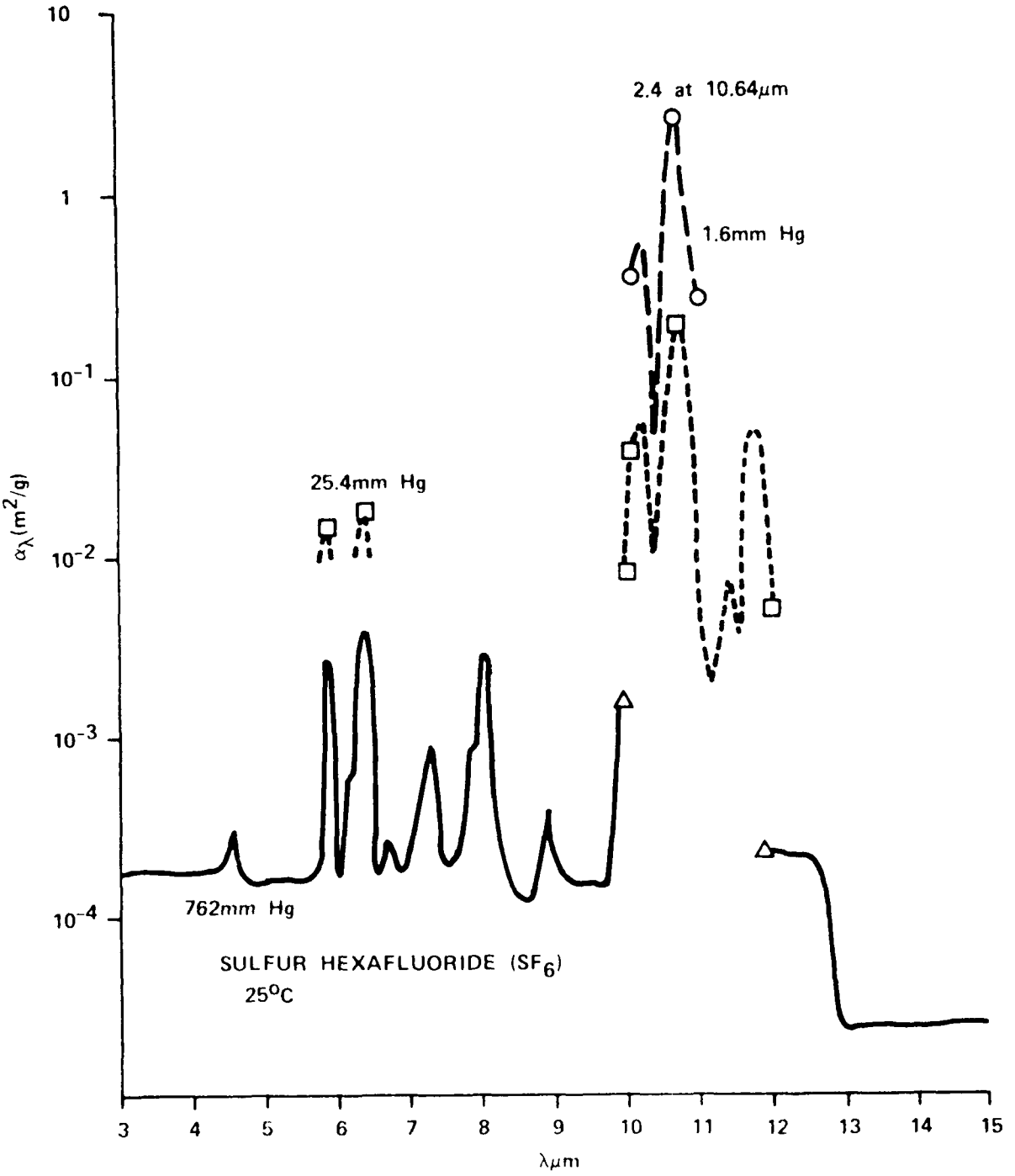

Figure B-1. Extinction (Absorption) Coefficients of Sulfur Hexafluoride (SF_6) Gas, 3-15 μm Wavelengths, 25 °C. Key: Solid curves and triangular points refer to 762-mm Hg sample pressure; short, dashed curves and square points refer to 25.4-mm Hg sample pressure; long, dashed curves with circular points refer to 1.6-mm Hg sample pressure. Samples were run in sealed cell to exclude atmospheric gases.

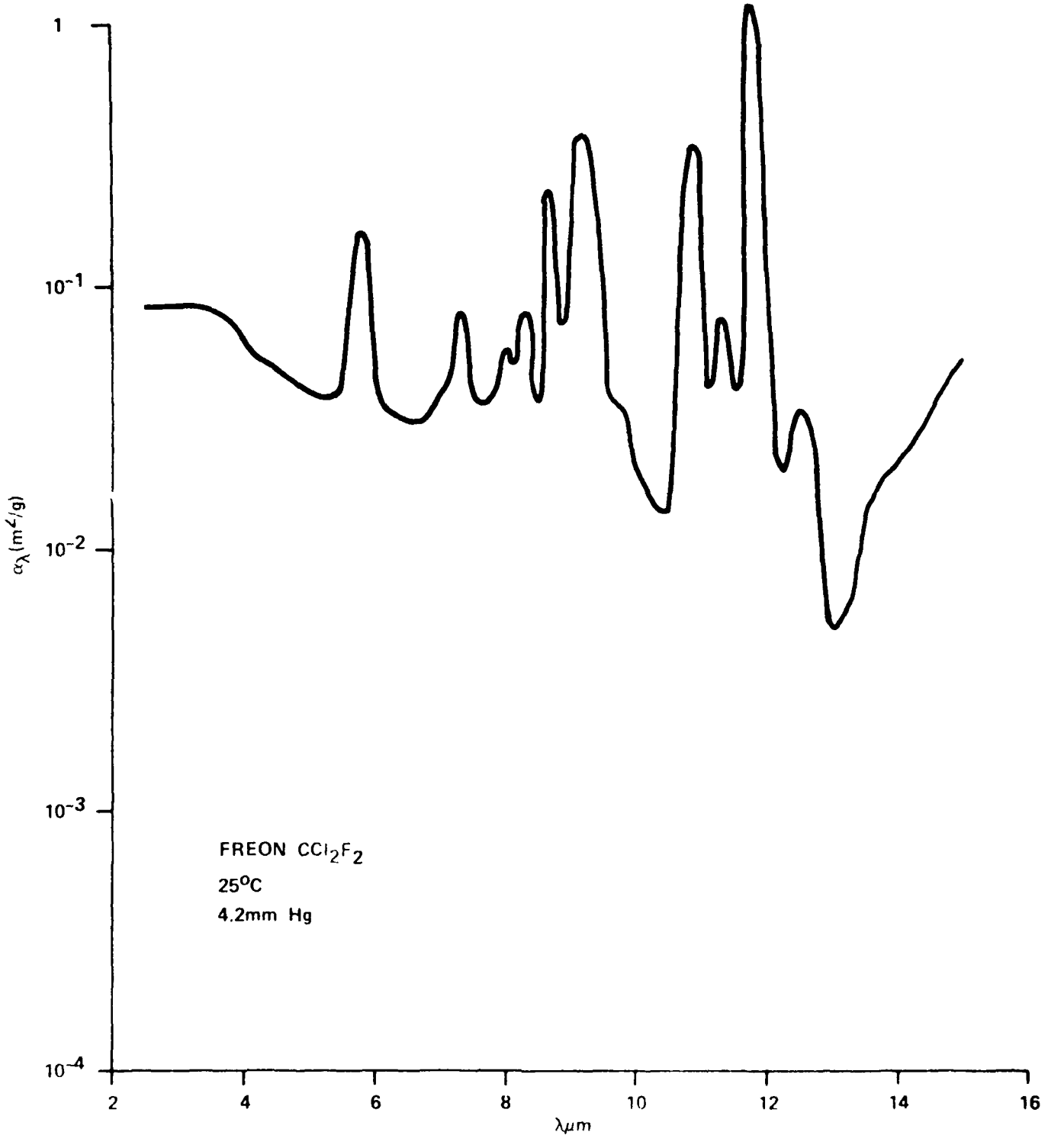

Figure B-2. Extinction (Absorption) Coefficients of Freon™ (CCl_2F_2) Gas, 3-15 μm Wavelengths, Partial Pressure = 4.2 mm Hg in 1 Atm Total Atmospheric Pressure at 25 °C.

The integrated absorption coefficients of Freon™ (4.2 mm Hg) or SF_6 (1.6 mm Hg) over the 8-13 μm IR window were both about 0.1 m^2/g or slightly less. This is comparable to the absorption coefficient of a water fog in this window (not including the scattering contribution to the total extinction coefficient).

Freon™ and SF_6 are commercially available in gas cylinders that facilitate their use in experiments. For example, a known weight of gas can be introduced into a test chamber simply by weighing the container before and after dissemination.[4] This is particularly easy if the container is not heavy (e.g., if Freon™ is taken from an aerosol can of electronic freeze mist). The volume of a chamber can be determined by introducing a known weight of gas into it and monitoring the IR transmission at an absorption peak over a known path. Or the path length (as in a multipass cell) can be approximated if the volume is known.

For atmospheric studies, extrapolation of the SF_6 data suggests that this gas could be detected using a CO_2-laser transmissometer at a partial pressure as low as about 10^{-5} mm Hg. This estimate is based upon typical levels of atmospheric water vapor absorption near λ = 10.6 μm. When aerosol extinction rather than water vapor absorption limits atmospheric transmission at this wavelength, the detectable partial pressure might be nearer 10^{-4} mm Hg. These estimates would, of course, have to be verified by actual observations.

B-4. CONCLUSIONS

The mass absorption coefficients for Freon™ and SF_6 presented in this report can be used qualitatively (e.g., in the wavelength calibration of a spectrometer or scanning radiometer), or semiquantitatively in a variety of practical applications, some of which are suggested. The absorption coefficients are directly comparable to the mass extinction coefficients of aerosols. Such comparison shows that the peak absorption coefficients of these gases at lower pressures can be comparable to or greater than those of strongly-attenuating aerosols including acid smokes and water fogs. But these gases have rather low integrated absorption coefficients over broad wavelength regions. For example, the integrated absorption coefficient over the 8-13 μm atmospheric window is 0.1 m^2/g for both gases at several measures of pressure related to mercury.

LITERATURE CITED

1. Carlon, H.R., Anderson, D.H., Milham, M.E., Tarnove, T.L., Frickel, R.H., and Sindoni, I., Infrared Extinction Spectra of Some Common Liquid Aerosols," Appl. Opt. Vol. 16, p 1598 (1977).

2. Lagemann, R.T., and Jones, E.A., J. Chem. Phys. Vol. 19, p 534 (1951).

3. Carlon, H.R., "Practical Upper Limits of the Optical Extinction Coefficients of Aerosols," Appl. Opt. Vol. 18, p 1372 (1979).

4. Carlon, H.R., "CL" Factors for Toxic Agents and Spectral Simulants Detected by Filter LOPAIR Equipment, CRDL Technical Memorandum 72-1, Edgewood Arsenal, MD, 1 Dec 1962, AD 472 170.

GLOSSARY

α_λ = optical extinction coefficient (or absorption coefficient for a gas) at wavelength λ, m^2/g.

C = mass concentration of gas or aerosol, g/m^3.

L_m = optical path length, m.

λ = wavelength of observation, μm.

M = molecular weight of gas, g.

p = partial pressure or sample pressure of gas, mm Hg.

T = optical transmittance at wavelength λ, unitless.

θ_k = absolute temperature, ^oK.